https://doi.org/10.1016/j.sna.2020.112270 Sensors & Actuators A, 2020

FEM exploration of the potential of silica diatom frustules for vibrational MEMS applications

Bakhodur Abdusatorov [1], Alexey I. Salimon [1], Yekaterina D. Bedoshvili [2], Yelena V. Likhoshway [2] and Alexander M. Korsunsky [1,3]*

[1] Hierarchically Structured Materials (HSM) laboratory, Center for Energy Science and Technology (CEST), Skolkovo Institute of Science and Technology, Moscow 121205, Russia
[2] Limnological Institute, Siberian Branch, Russian Academy of Sciences, 3 Ulan-Batorskaya St., Irkutsk, Russia 664033
[3] MBLEM, Department of Engineering Science, University of Oxford, Parks Road, Oxford OX1 3PJ
* Correspondence: alexander.korsunsky@eng.ox.ac.uk; Tel.: +44 1865 2 73043

Abstract: Numerical simulations were carried out using the Finite Element Method (FEM) to determine the frequency characteristics of mechanical vibration of diatom silica frustules under the conditions and at frequencies that are not readily accessible to experimental measurement. The results revealed the influence of the frustule morphology on the natural frequency spectra. The effect of frustule density, stiffness, dimensions, pore size, and wall thickness on the eigenfrequencies and the corresponding modal shapes were studied in detail. Diatom frustules have natural frequencies in the range between several MHz and tens of MHz that make them a promising candidate for future MEMS applications. Eigenfrequencies depend linearly on the speed of sound in the frustule wall and decrease parabolically with the diameter and the pore size to diameter ratio. Dimensional analysis allowed obtaining functional correlations that encapsulate the various dependencies in compact analytical form. The satisfactory nature of our calculations and correlations derived from them is confirmed through an agreement with the analytical solutions from the literature.

Keywords: Diatoms; Bio-inspired Materials; Finite Element Analysis, Natural frequencies

1. Introduction

The biological class of diatomic algae is an example of nature's fascinating collection of intricate hierarchical architectures of exoskeletons (known as frustules) that are optimized for functional and structural performance at multiple length scales, and produced in a cheap and environmentally friendly way in the volume that vastly exceeds that of artificially manufactured nanostructured materials [1,2]. Diatoms, a class of single-cell algae found in aquatic environments have millions of unique species with distinct morphologies of frustules made from amorphous hydrated silica [3]. Depending on symmetry diatoms are usually classified into two groups: centric (often circular) and pennate (elongated) (Figure 1). Extraordinary mechanical properties, such as high deformability and high specific strength [4], are combined with the ability of biological reproduction even in Antarctic temperatures (below freezing) [5], making diatoms a unique instance of natural nano-fabrication at the global scale. The manipulation and genetic control of diatom frustule nano-structuring could revolutionize the device fabrication routes for energy storage, optoelectronics, solar cells [6], and batteries [7]. Diatoms have intricate intrinsic features: biocompatibility, unique nano-pore arrangement, specific surface area and mechanical strength. In recent decades they have been proposed for use in drug delivery [6-8], microfluids [9,10], batteries [11-12], templates [13-15], biosensors [16-17], for energy conversion and storage [18]. Diatoms used as a platform for nanotechnology hold a crucial advantage over photolithography because they multiply in geometric progression, i.e. at a much faster rate than is possible for any technology of fabrication for MEMS [18] and in which is faster than the manufacturing speed of MEMS. This bioinspired silica can be used directly or in modified form in design for specific properties. Diatoms have rigid surfaces in relative motion, and their tribology has a high potential regarding 3D MEMS [19]. Some studies of the mechanical properties of diatom frustules have been reported in the literature. The mechanical vibration behaviour of diatom frustules is important because their small size, light weight and high stiffness lead to the expectation of them having high

natural vibration frequencies with potential applications in MEMS, especially considering the diversity of sizes and shapes that diatoms offer. The Finite Element Method offers a suitable analysis technique for the study of mechanical properties of small biomaterials. The mechanical properties of diatoms are widely studied in the literature [4]. In particular, computer modeling has become an increasingly popular approach to the study of biomaterials with complex structure at the nano- and micro- scales. Hamm et al. performed Finite Element Analysis of *Fragilariopsis kerguelensis* frustules and showed that diaphragmatic grooves have high rigidity of about 9.8 GPa [4]. The authors considered that diatoms obtained their unique architecture as a result of a long evolutionary process under the influence of environmental factors, in order to optimize such properties as protection from predators. Several studies attempted to analyze diatom frustule structere in the context of hierarchical design by Nature. Moreno *et al*. studied the relationship between porosity and mechanical properties [21]. Similarly, Gutiérrez *et al*. investigated the effect of morphological features (such as the diameter of diatoms, pore size and thickness of individual walls) on the deformation response of centric diatoms [22]. It remains extremely challenging, if not impossible to simulate the real structure of diatoms. Several studies have shown the most considerable importance of pore size for the properties of diatom frustules. Yuan Xing proposed the use of Focused Ion Beam - Scanning Electron Microscopy (FIB-SEM) as a powerful tool for the systematic 3D study of the morphological features of diatoms on the basis of a series of high-resolution images [23]. Lu el. reported high precision simulation of *Coscinodiscus sp.* valve, starting with a unit cell that included three layers of the valve (*hole*, *cribrum* and *cribellum*) and even taking into account the curvature of the pore walls of the hole (*areola* chambers) [24]. Meza et al. made a significant advance in additive manufacturing complex microarchitectural materials down to the nanometer precision. *In situ* nanomechanical testing showed high strength and stiffness, and near complete recovery (up to 98%) after large compression up to ≥50% [25]. More recently, E. Topal *et al*. used the combination of X-ray computed tomography (XCT), FEM analysis and micro-scale testing to study the mechanical response to *Didymosphenia geminata fidula*. They were able to obtain accurate 3D morphological data for model input. The limited XCT resolution of 130 nm meant that SEM was used to define nanopore size and shape. Effective Young's Modulus of the frustule was determined to be 31.8 GPa, significantly lower than bio-silica (70 GPa) due to porosity, as is the case for many biological materials with hierarchical structure.

In the present study, we focus our attention on the numerical study of the effect of morphology and material properties of diatom frustules on the mechanical vibration behaviour. The type of diatoms was selected based on the ordered arrangement of pores and symmetry. Symmetry alleviates simulation analysis and visualization. *Coscinodiscus sp.* (centric) and *Synedra acus* (pennate) diatom species satisfy the criteria above. Their slim nanostructures can be integrated into nanodevices, which is the strategic focus of our study. The main objective of our research is to explore diatom's potential for MEMS, namely, oscillators or vibrational sensors able to resonate at eigenfrequencies detecting specific external vibration. Our scientific group recently managed to make other steps towards this goal, namely, to achieve guided colonization of Si wafers with diatoms [21] and to reduce natural diatom opal to obtain nanostructured Si objects while retaining neat nanostructure [22]. These steps are being theoretically and conceptually supported by the modelling presented in this manuscript.

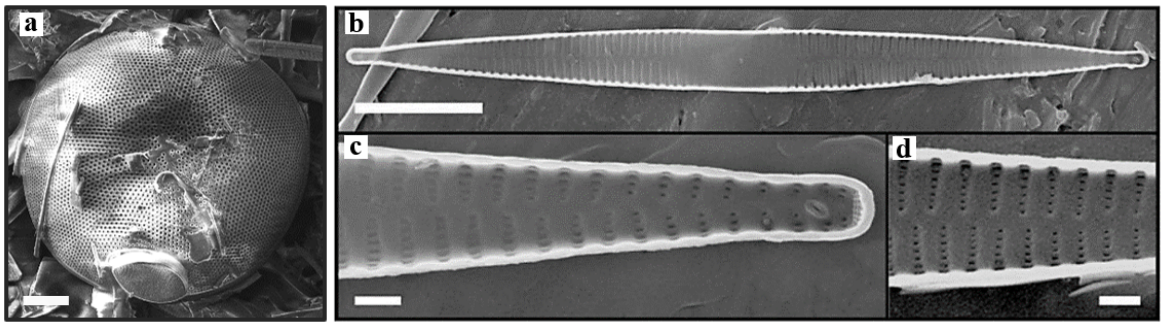

Figure 1 SEM images of (a) a centric diatom frustule and (b, c, d) pennate *Synedra acus* frustules [23]. Scale bar: 10 μm

1.1. The frustules of *Coscinodiscus sp.* and *Synedra acus*

Coscinodiscus sp. and *Synedra acus* diatoms represent the extremes in terms of taxonomy and, as one can see, topology as well. Centric diatoms can be considered as quasi-spherical thin shells (or domes) fundamentally and thoroughly studied in continuous mechanics. The issues of porosity and height-to-diameter aspect become crucial for eigenfrequencies. Pennate diatoms depending on the width-to-length aspect may be treated as close to centric or, like for the considered *Synedra*, as slender rod or beam, or even as elastic continuous string. Theoretical models for long rods or elastic strings are also well documented in scientific literature and simplest formulae can be applied for fast estimations. Porosity can be accounted for as reduction factors for density and stiffness. Diatom frustules consist of 10 to 70% amorphous silica with the density not exceeding 2600 kg/m^3, and the remaining organic components such as proteins with the density of 1300 kg/m^3, and polysaccharides of 1070 kg/m^3. Therefore, frustule densities can range from 1400 kg/m^3 to 2200 kg/m^3, according to literature [24]. The frustules of diatom algae consist of two halves, known as valves. In the case of *Coscinodiscus sp.* with centric symmetry (Fig.1a) the shape of each valve is remindful of a Petri dish with the diameter ranging from 50 to 200 μm, and the dome height of 12 μm. A system of holes or pores with the diameters of 0.4 μm to 2.6 μm penetrate the frustule from the concave to the convex surface. The valves that are joined by the surrounding circular girdle band of about 3 μm width. The thickness of the silica frustule walls varies from 0.2 to 2 μm [20]. In previous studies, nanoindentation of *Coscinodiscus sp.* revealed the material stiffness of 22.4 GPa [4], which is comparable to that of the cortical bone (20 GPa) [25], but is significantly lower than that of bulk silica glass (73 GPa) [26] perhaps due to the presence of both organic binder and nanometer size porosity. *Synedra acus* with the structure illustrated in Fig.1b is a class *Fragilariophyceae* that is abundant in ground water. It was chosen as representative of the pennate group of diatoms that display bi-fold symmetry. Pennate diatoms typically have the form of elongated ellipsoids consisting of the upper valve (epitheca) and lower valve (hypotheca) joined by the girdle band. Each half shell consists of ribs (costae) with orifices classified according to their location and size into raphe (central longitudinal ridge), striae and areolae. The cell culture was isolated from the natural population endemic in Lake Baikal and was allowed to grow naturally in a plastic contained placed on a laboratory windowsill.

2. Methodology

2.1. 3D CAD and FEA modeling of hierarchically structured frustules

The numerical simulations carried out in the current project studied the dependence of vibration properties on a range of parameters, namely, the overall frustule geometry, the dimension of characteristic features, and material properties. Additionally, the mesh size effect was considered to ensure the reliability of results. At the start of the simulation, a three-dimensional CAD model was created using SolidWorks software version SP5.0. The model was constructed based on the actual morphology and dimensions of frustules obtained using Scanning Electron Microscopy (SEM). For the purposes of implementation within numerical simulations, the frustule geometry was simplified (Fig.2). The objects simulated were single valves in the form of perforated domes with vertical band at the rim. Real diatom frustules may consist of several distinct layers of silica, and the overall frustule thickness may not be constant around pores and orifices. However, for the purposes of obtaining systematic estimates, in this research we considered the frustules to be uniform and single layer. Although therefore this does not provide a detailed reconstruction of the real intricate geometry of diatom

frustule, the key aspects of geometry and hence mechanical response were captured with appropriate reliability, whilst the approximations chosen allowed reducing the computational time and performing parametric study to derive the correlations sought. The 3D modelling process ran as follows. Firstly, a 2D cross-sectional model of one valve of the diatom frustule was designed according to the typical dimensions of *Coscinodiscus sp.* taken from previous studies [20,24]. Subsequently, this cross section was 'swept' around the axis to obtain a body of rotation with centric symmetry. To model the wall structure seen in SEM images, pores were added. For the constructing a geometric model of *Synedra acus*, dimensions were taken from the work of Basharina et al. [23]. Parametric simulation studies of the frustule vibrational properties were carried out by fixing all variable parameters with the exception of one that was varied to obtain the dependence.

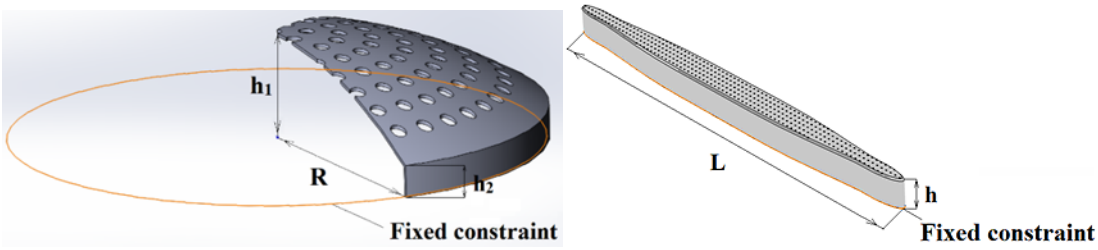

Figure 2 Model geometry (a) of centric diatom *Coscinodiscus sp.* with the diameter D = 50µm, total height h_1 = 10 µm, rim height h_2 =3 µm, and wall thickness t =0.3 µm (b) A model of pennate *Synedra acus* with the length L = 160 µm, height h = 4.5 µm, and width w = 6 µm, respectively.

2.2. FEM simulation

FEM simulations of natural frequencies were conducted using COMSOL Multiphysics Version 5.4, Structural Mechanics module. The mesh consisted of between 40,000 and 70,000 tetrahedral elements depending on the geometry and pore size of diatoms, and mesh refinement. The diatom model was fixed at the girdle band location, with all displacement components set to zero. The values of Young's modulus E, Poisson's ratio ν and density ρ were taken from previous studies [4,24,27] (Table 1).

TABLE 1
DIATOM MODEL PARAMETERS

Material Properties	Elastic Modulus (E)	22.4 GPa
	Density (ρ)	2200 kg/m^3
	Poisson's ratio (ν)	0.17
Coscinodiscus sp.	Radius	25 µm
	Total height	10 µm
	Rim height	3 µm
	Pore size	1.5 µm
	Thickness of walls	0.3 µm
Synedra acus	Length	160 µm
	Width	6 µm
	Height	4.5 µm
	Pore size	0.3 µm

3. Results

3.1. Analysis of the results

For the purposes of evaluating the suitability of diatom frustules for MEMS applications as vibration elements, the key requirement concerns the ability to predict the eigenfrequency values based on the frustule size, shape, and mechanical characteristics.

3.2. Modal shapes

The shapes of first six vibration modes are illustrated in Fig. 3. For *Coscinodiscus sp.* the displacements mapped correspond to the direction along the symmetry axis of the valve. For *Synedra acus*. the displacements shown are normal to the plane of the girdle band. The vibration mode shapes for the centric diatom valve are similar to those of a circular plate [28,29], whilst for the pennate diatom *Synedra acus.* they are similar to that of an extended rod. Fig.3 illustrates the maximal deflection shapes displayed by the lowest six distinct natural vibration modes for the two types of diatom frustules considered.

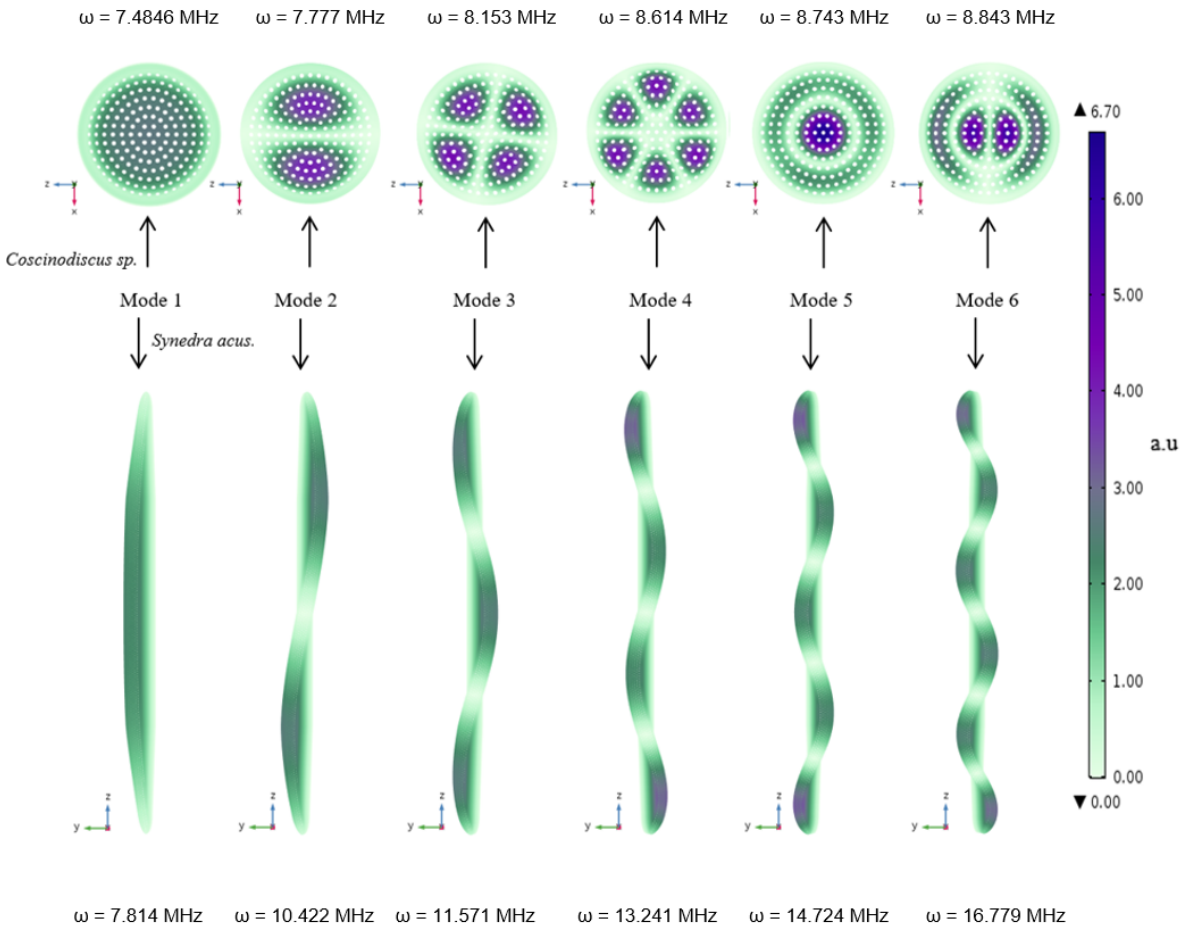

Figure 3 Mode shapes and natural frequencies of *Coscinodiscus sp.* (centric) and *Synedra acus.* (pennate) observed in the simulation using COMSOL Multiphysics.

The variation of vibration eigenfrequency with the mode number is illustrated in Fig.4 and shows approximately linear dependence

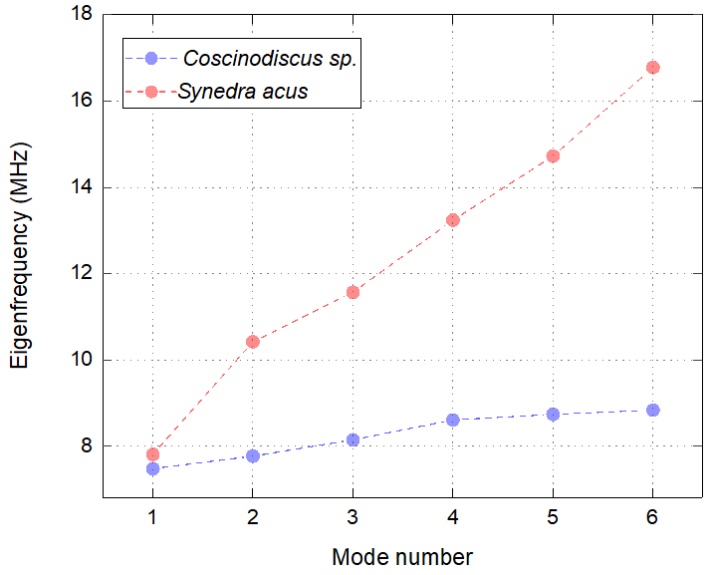

Figure 4 The dependence of the natural vibration mode eigenfrequency on the mode number.

Whilst numerical modelling is required in each specific case, the fundamental relationship between diatom properties and vibration eigenfrequencies can be conveniently expressed in functional form that we refer to as 'correlation' here, to distinguish it from analytical models that can be derived mathematically – albeit with great difficulty [29,30].

In seeking the form of the correlation, we begin with the assumption that the i-th eigenfrequency of mechanical vibration depends on the following parameters:

$$\omega_i = F_i\,(E, \rho, D, t, d). \tag{1}$$

Here D is diameter of the frustule, d the pore diameter (also referred to as *pore size* below, and used interchangeably), t frustule wall thickness, E is Young's Modulus, and ρ is density. In the case of *Coscinodiscus sp.* centric diatom frustules, detailed parametric analysis was carried out to determine the functional form of the sought correlation. To ensure reliability of the results, mesh density was increased to obtain apparent convergence. The lowest six vibration modes were taken into consideration in the first instance. It was found that for the highly symmetric centric diatom shape some modes with distinct geometric modal shape corresponded to the same frequency. There were some frequency coincidences for higher order modes as well. In the charts shown below four distinct modes are studied in detail.

3.1.1. The effect of Young's Modulus E

Fig. 5 illustrates the linear proportional increase eigenfrequency with the square root of Young's modulus. This stiffness parameter is likely to be modified to some extent via careful heat treatment that should reduce nanometer size porosity or cause such transformations like elimination of hydrate water or devitrification (crystallization towards quartz or cristobalite) while retaining structure porosity unchanged. This approach promises a degree of control over MEMS working parameters.

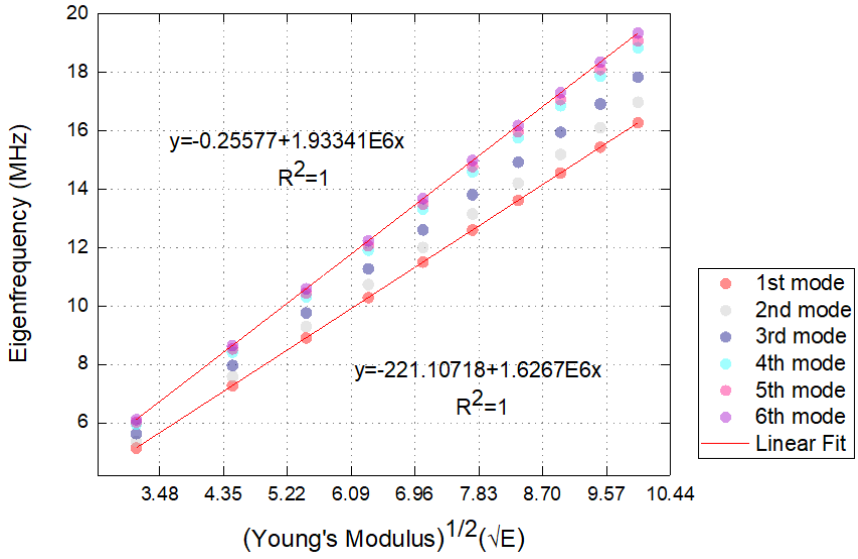

Figure 5 The effect of material stiffness (plotted as the square root of Young's modulus on the horizontal axis) on the eigenfrequency of the hemispherical shell (pore diameter d was fixed at 1.5 μm).

3.1.2. The effect of density ρ

Figure 6 illustrates that the natural frequency of frustule vibration increases linearly with the inverse square root of material density that was varied between 1400 to 2200 kg/m^3 in this study.

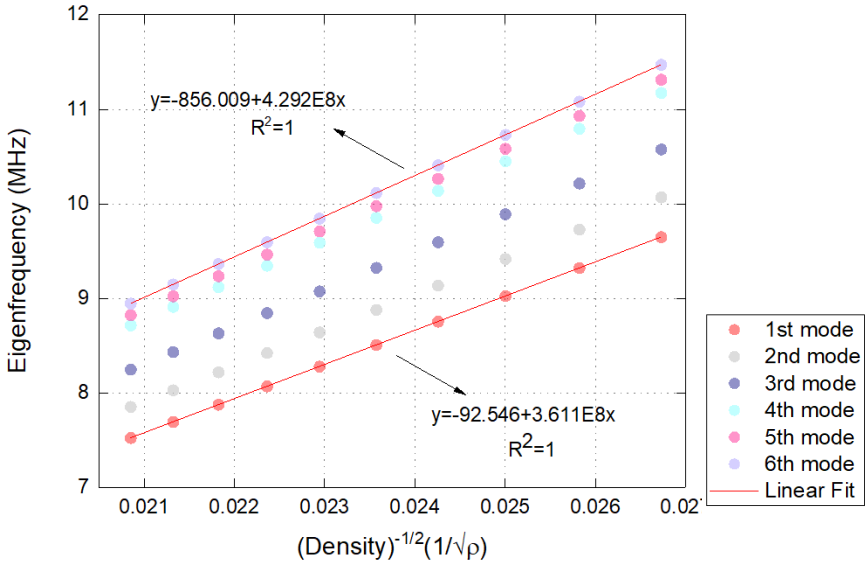

Figure 6 The linear proportional dependence of eigenfrequencies on the inverse square root of material density

3.1.3. The effect of frustule diameter D

Simulations were performed for the frustule diameter D in the range between 40 and 200 μm, which covered all instances of *Coscinodiscus sp.* reported. In these simulations, the heights of the dome, the rim and pore diameter were variable. Material properties and the number of pores were constant. Fig.7 shows that the resulting correlation between frequency and inverse diameter 1/D can be successfully approximated with a quadratic linear constrained to pass through the origin, indicating that the vibration frequency becomes approaches zero asymptotically as the frustule diameter tends to infinity. As the diameter of the diatom frustule decreases, the eigenfrequency increases quadratically. It is also worth noting that the eigenfrequency values for different modes considered lie close to each other, differing by about 20%.

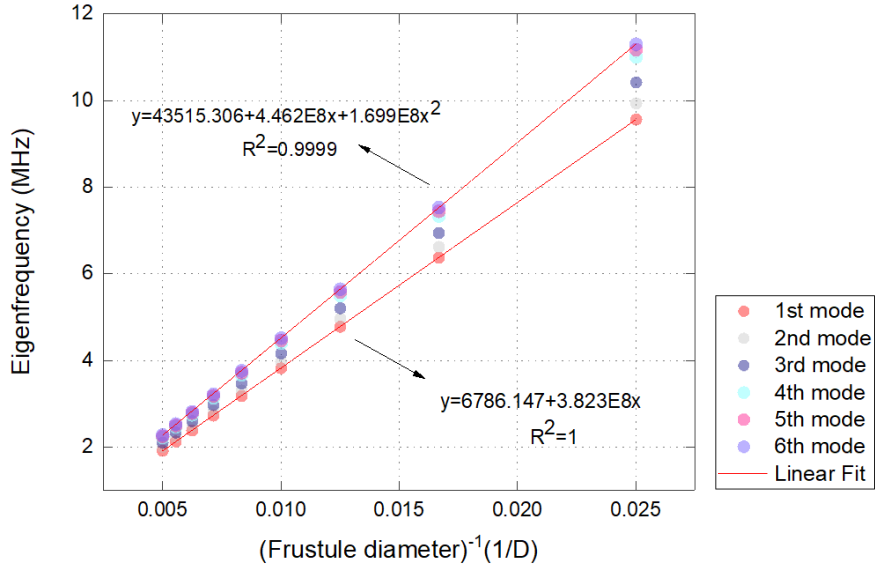

Figure 7 The (weakly) quadratic dependence of vibration eigenfrequencies of a centric diatom frustule on the inverse frustule diameter 1/*D*.

3.1.4. The effect of frustule walls thickness t

Simulations of the effect of wall thickness were performed with all parameters fixed, and wall thickness t varied in the range between 0.2 and 2.0 μm. The variation of frequency parameters with the wall thickness is moderate, with the change by a factor of 2 approximately over a decade of thickness variation. The dependence is described well by a polynomial function, as illustrated in Fig. 8.

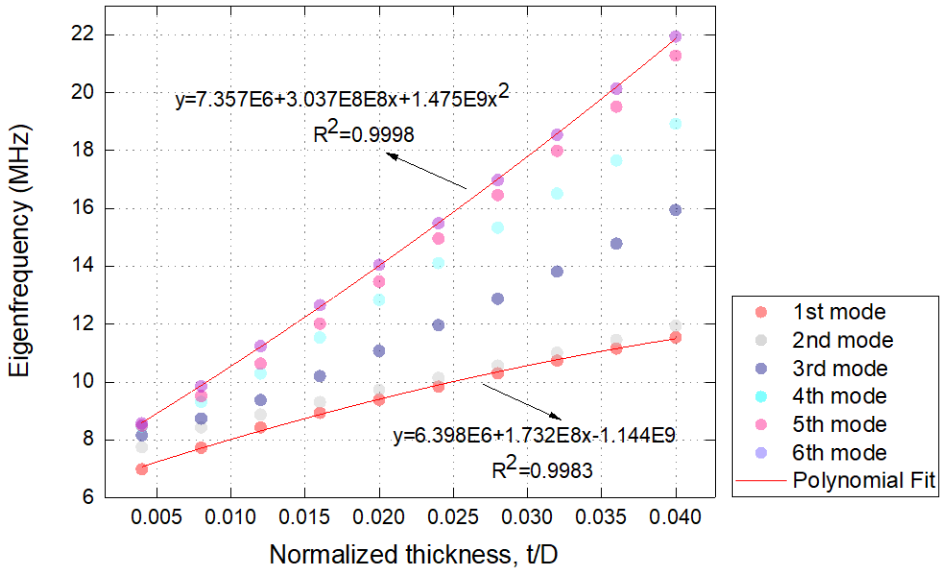

Figure 8 The effect of normalized wall thickness, *t*/*D*, on the frustule vibration eigenfrequency.

3.1.5. The effect of pore diameter d

The simulations were performed for a wide range of pore diameter. For all calculations, the position and number of pores were fixed (N=233). Fig. 9 Illustrates the decrease of frustule eigenfrequency as the pore diameter d increases. The distance between pores, the number and positions of pores were fixed. For the models considered, the pore diameters varies from 0.4 μm to 2.6 μm, with a step 0.2 μm. It appears that the normalized pore diameter, (d/D), exerts a strong influence on vibration frequency that is distinct for different modes. It appears that in all cases the variation could be well described by the polynomial approximation

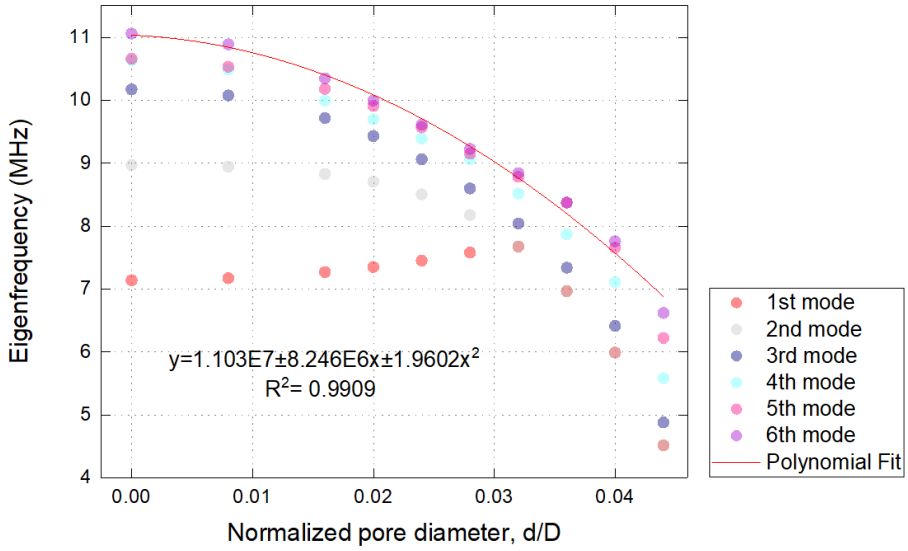

Figure 9 The eigenfrequency dependence on the normalized pore diameter of the *Coscinodiscus sp.* frustule, *d*/*D*.

3.3. Synthesis: the correlation expression for frustule eigenfrequencies

Finite Element Modelling results shown above can be collated into the functional form of correlation between i-th mode eigenfrequency and frustule parameters, as follows.

$$\boldsymbol{\omega_i} \propto \sqrt{\frac{\boldsymbol{E}}{\boldsymbol{\rho}}}. \tag{2}$$

This is in agreement with the behavior expected from shell vibration theory.

Dimensional analysis requires that vibration frequency (units of Hz, s^{-1}) must be expressed in terms of the speed of sound through division by a linear dimension of the shell. We choose to express this in terms **of the shell diameter *D* as follows**:

$$\boldsymbol{\omega_i} \propto \sqrt{\frac{\boldsymbol{E}}{\boldsymbol{\rho}}}\frac{\mathbf{1}}{\boldsymbol{D}}. \tag{3}$$

From Fig. 7 and Fig. 8 one may note, however, that the eigenfrequency dependence on the inverse diameter is quadratic, of the following specific form

$$\boldsymbol{\omega_i} \propto \boldsymbol{a_i}\, \boldsymbol{t}\, \boldsymbol{x^2} + \boldsymbol{b_i x}, \tag{4}$$

where $\boldsymbol{x} = \mathbf{1}/\boldsymbol{D}$. This can be combined with (3) to obtain the following expression:

$$\boldsymbol{\omega_i} \propto \sqrt{\frac{\boldsymbol{E}}{\boldsymbol{\rho}}}\frac{\mathbf{1}}{\boldsymbol{D}}\left[\boldsymbol{a_i}\frac{\boldsymbol{t}}{\boldsymbol{D}} + \boldsymbol{b_i}\right]. \tag{5}$$

Note that the relative thickness parameter $\boldsymbol{t}/\boldsymbol{D}$ was used here to obtain the required dominant quadratic dependence of frequency on the inverse diameter $\mathbf{1}/\boldsymbol{D}$.

Finally, as shown in Fig. 9, the dependence of eigenfrequency on the pore diameter d can be expressed in a polynomial form, which can be cast in terms of the normalized ratio (d/D), leading to the following overall correlation expression:

$$\boldsymbol{\omega_i} \propto \sqrt{\frac{\boldsymbol{E}}{\boldsymbol{\rho}}}\frac{\mathbf{1}}{\boldsymbol{D}}\left[\boldsymbol{a_i}\frac{\boldsymbol{t}}{\boldsymbol{D}} + \boldsymbol{b_i}\right]\boldsymbol{P_i}\left(\frac{\boldsymbol{d}}{\boldsymbol{D}}\right). \tag{6}$$

Expression (6) provides a compact and easily useable correlation between eigenfrequency and diatom frustule materials and morphological parameters and can help guide the selection and design of MEMS vibration elements using frustule fabrication.

4. Comparison between numerical simulations and analytical solution

To confirm the reliability of our results, we used the analytical results of Shang [31]. Using the Naghdi-Reissner shell theory and Legendre functions, an analytical solution was obtained for vibration frequencies of spherical-cylindrical shells that was expressed in the form:

$f = \frac{1}{2\pi R}\sqrt{\lambda E/\rho(1-v^2)}$, that can be re-written in our notation as $\omega \propto \frac{1}{D}\sqrt{\frac{E}{\rho}}\sqrt{\lambda(t,d)}$ and compared with our result: $\omega_i \propto \frac{1}{D}\sqrt{\frac{E}{\rho}}\left[a_i\frac{t}{D} + b_i\right]P_i\left(\frac{d}{D}\right)$.

It can be seen from above that the principal leading terms $\sqrt{\frac{E}{\rho}}\frac{1}{D}$ are captured correctly. The term denoted by Shang [31] as $\sqrt{\lambda(t,d)}$ that accounts for morphological details of the shell, in our notation is given by $\left[a_i\frac{t}{D}+b_i\right]P_i\left(\frac{d}{D}\right)$, benefitting from the more precise and specific identification of dependence on *t* and *d*.

More detailed matching of numerically derived correlations to analytical solutions is unrealistic, for several reasons:

- an analytical solution could only be found for a hemispherical shell (in fact, attached to a cylindrical shell to form a "capsule")
- obtaining an analytical solution for a smaller segment of a sphere is even more challenging; and harder still (if not impossible) is to incorporate the effect of holes

The hallmark of our approach is that it manages to overcome the challenge of combining FEM with rational dimensional analysis and correlation derivation. This is in line with the current emphasis on using computation to determine underlying relationships in the context of Machine Learning and Artificial Intelligence.

5. Conclusions

The natural vibration frequencies of two different diatom frustule shapes were analysed, centric *Coscinodiscus sp.* and pennate *Synedra acus.* For the former centric shape in particular it was revealed how the natural frequencies depend on the frustule morphological features, such as material stiffness and density, valve diameter, wall thickness, and pore diameter. Diatom frustules are expected to have vibration frequencies in the MHz range. Bio-silica low density and high Young's Modulus make diatom frustules outstanding candidates for MEMS applications. It has been shown that the natural frequencies increase with the decrease of diatom's diameter scale, pore size and density, while at low Young's Modulus and thickness the eigenfrequency decreases. We proposed simple solution method for a natural vibration analysis of diatom frustules, regardless of the shapes. The analytical solution of spherical-cylindrical shells and solution obtained from FEA were compared with each other and the present results in good agreementıo FEM can produce a good approximate solution. The strategic direction of enquiry presented in this paper may pave the way towards controlled MEMS bio-fabrication, in the present case via diatom frustules. Diatom frustule simulation performed in the article will help to guide the selection and adoption of specific diatoms that can be applied for mass production of low-cost devices at the micro and nanoscale.

Conflicts of interest

Authors have no conflicts to declare.

Acknowledgements

AMK wishes to acknowledge funding support from the Royal Society (UK) under project IEC/R2/170223.

6. References

[1] Xiaorong, X.; Mary, E. L.; Babak, A. P. Microorganisms for MEMS. *J. MEMS* **2007**, *16*, 429-444. doi: 10.1109/JMEMS.2006.885851.

[2] Wang, Y.; Cai, J.; Jiang, Y.; Jiang, X.; Zhang, D. Preparation of biosilica structures from frustules of diatoms and their applications: current state and perspectives. *Appl. Microbiol. Biotechnol.* **2013**, *97*, 453–60. doi: 10.1007/s00253-012-4568-0.

[3] Round, F.E.; Crawford, R.M.; Mann, D.G. *The diatoms: biology and morphology of the genera*, Cambridge University Press 1990 https://doi.org/10.1017/S0025315400059245.

[4] Hamm, C.E.; Merkel, R.; Springer, O.; Jurkojc, P.; Maier, C.; Prechtel, K. and Smetacek, V., Architecture and material properties of diatom shells provide effective mechanical protection, *Nature,* **2003**, *421*, 10441- 10444, https://doi.org/10.1038/nature01416.

[5] Gordon, R.; Witkowski, A.; Gebeshuber, I.C.; Allen, C.S., *The diatom of Antarctica and their potential roles in nanotechnology*. In: Masó M., editor. Antarctica. Time of Change. Editions ACTAR; Barcelona, Spain:2010. pp. 84-95.

[6] Delalat, B., Sheppard, V., Rasi Ghaemi, S. et al. Targeted drug delivery using genetically engineered diatom biosilica. *Nat. Commun.* 6, 8791 (**2015**). https://doi.org/10.1038/ncomms9791

[7] Delasoie, J.; Zobi, F. Natural Diatom Biosilica as Microshuttles in Drug Delivery Systems. *Pharmaceutics* **2019**, 11, 537, doi: 10.3390/pharmaceutics11100537

[8] Kabir, A.; Nazeer, N; Bissessur, R.; Ahmed, M., Diatoms embedded, self-assembled carriers for dual delivery of chemotherapeutics in cancer cell lines, *Int. J. Pharm*., **2020**, Volume 573, 118887, https://doi.org/10.1016/j.ijpharm.2019.118887

[9] Kim, K., Liang, Z., Liu, M., & Fan, D. "Emma.". Biobased High-Performance Rotary Micromotors for Individually Reconfigurable Micromachine Arrays and Microfluidic Applications. *ACS Appl. Mater.*, **2017,** 9(7), 6144–6152. doi:10.1021/acsami.6b13997

[10] Jarrett, H., Wade, M., Kraai, J. et al. Self-powered microfluidic pump using evaporation from diatom biosilica thin films. Microfluid Nanofluid 24, 36 (**2020**). https://doi.org/10.1007/s10404-020-02343-5

[11] Campbell, B., Ionescu, R., Tolchin, M. *et al.* Carbon-Coated, Diatomite-Derived Nanosilicon as a High Rate Capable Li-ion Battery Anode. *Sci Rep,* **2016,** 6**,** 33050, https://doi.org/10.1038/srep33050

[12] Andreas Nicolai Norberga, Nils Peter Wagnerab, Henning Kalanda, Fride Vullum-Bruerc and Ann Mari Svensson, Silica from diatom frustules as anode material for Li-ion batteries, doi:10.1039/C9RA07271C RSC Adv., **2019**, 9, 41228-41239

[13] **2016** DOI: 10.1038/ncomms13440

[14] (**2017**) https://doi.org/10.1088/1361-6463/aa63b0

[15] Li, K., Liu, X., Zheng, T., Jiang, D., Zhou, Z., Liu, C., … Losic, D. (**2019**). Tuning MnO2 to FeOOH replicas with bio-template 3D morphology as electrodes for high performance asymmetric supercapacitors. Chemical Engineering Journal. doi:10.1016/j.cej.2019.03.190

[16] Cai, J., Pan, J. F., Chen, M. L., Wang, Y., & Zhang, D. Y. (**2013**). Culturing and Bonding of Diatom on a Microfluidic Chip for Biosensing Application. Applied Mechanics and Materials, 461, 809–813. doi:10.4028/www.scientific.net/amm.461.809

[17] Yang, J.; Zhen, L.; Ren, F.; Campbell, J.; Rorrer, G. L.; Wang, A. X. Ultra-sensitive immunoassay biosensors using hybrid plasmonicbiosilica nanostructured materials. J. Biophotonics. **2015**, 8, 659−667.

[18] Sun, X.W.; Zhang, Y.X.; Losic, D. Diatom silica, an emerging biomaterial for energy conversion and storage. J. Mater. Chem. A **2017**, 5, 8847–8859

[19] Terracciano, M.; Napolitano, M.; De Stefano, L.; De Luca, A.C.; Rea, I. Gold decorated porous biosilica nanodevices for advanced medicine. Nanotechnology 2018, 29, 235601

[20] Yang, J.; Zhen, L.; Ren, F.; Campbell, J.; Rorrer, G. L.; Wang, A. X. Ultra-sensitive immunoassay biosensors using hybrid plasmonicbiosilica nanostructured materials. J. Biophotonics. **2015**, 8, 659−667.

[21] Miguel, M.; Kaka, M.; Julie, S.; Lilian, D., An Integrated Approach for Probing the Structure and Mechanical Properties of Diatoms: Toward Engineered Nanotemplates, *Acta biomaterialia*., **2015**, 25, 313-24. doi: 10.1016/j.actbio.2015.07.028.

[22] Alejandro, G., Metin, G.; & Fedder, Gary & Dávila, Lílian. The Role of Hierarchical Design and Morphology in the Mechanical Response of Diatom-inspired Structures via Simulation. Biomaterials Science. (2017) 6. doi: 10.1039/C7BM00649G.

[23] Xing Y, Yu L, Wang X, Characterization and analysis of Coscinodiscus genus frustule based on FIB-SEM et al.Progress in Natural Science: Materials International (**2017**) 27(3) 391-395 doi: 10.1016/j.pnsc.2017.04.019

[24] lu, Jie & Sun, Cheng & Wang, Qian. (2015). Mechanical Simulation of a Diatom Frustule Structure. Journal of Bionic Engineering. (2015), 12. 10.1016/S1672-6529(14)60104-9.

[25] Lucas R. Meza, Alex J. Zelhofer, Nigel Clarke, Arturo J. Mateos, Dennis M. Kochmann, and Julia R. Greer PNAS September 15, 112 (37) 11502-11507; September 1, 2015 https://doi.org/10.1073/pnas.1509120112

[26] Peter Fratzl, Richard Weinkamer, Nature's hierarchical materials, Progress in Materials Science, Volume 52, Issue 8, **2007**, Pages 1263-1334, ISSN 0079-6425, https://doi.org/10.1016/j.pmatsci.2007.06.001.

[27] Topal, E.; Rajendran, H.; Zgłobicka, I.; Gluch, J.; Liao, Z.; Clausner, A.; Kurzydłowski, K.J.; Zschech, E. Numerical and Experimental Study of the Mechanical Response of Diatom Frustules. Nanomaterials **2020**, 10, 959.

[28] Sinha, S.K.; Satyanarayana, N.; Lim, S.C. Nano-tribology and Materials in MEMS, *Springer*, New York, 2013, doi: 10.1007/978-3-642-36935-3

[29] Gutierrez, A.L.; Gordon, R.I.; Davila, L.P., Deformation modes and structural response of diatom frustules, *J. Mater. Sci. Eng. Adv. Technol*, **2017**, *15*, 105-134, doi: http://dx.doi.org/10.18642/jmseat_7100121810.

[30] Salimon, A.I.; Everaerts, J.; Sapozhnikov, P.V.; Statnik, E.S. and Korsunsky, A. M. On Diatom Colonization of Porous UHMWPE Scaffolds, Proc. Wld. Cong. on Eng. WCE 2018, Vol. 2, http://www.iaeng.org/publication/WCE2018/WCE2018_pp695-699.pdf

[31] Aggrey, P; Abdusatorov, B; Kan, Y; Salimon, I.A. Lipovskikh, S.A.; Luchkin, S; Zhigunov, D.M.; Salimon, A.I. and Korsunsky, A.M. In Situ Formation of Nanoporous Silicon on a Silicon Wafer via the Magnesiothermic Reduction Reaction (MRR) of Diatomaceous Earth, *Nanomaterials,* **2020**, 10(4), 601 https://doi.org/10.3390/nano10040601

[32] Basharina, T. N.; Danilovtseva, E. N.; Zelinskiy, S. N.; Klimenkov, I. V; Likhoshway Y. V., Annenkov, V. V., The Effect of Titanium, Zirconium and Tin on the Growth of Diatom *Synedra Acus* and Morphology of its Silica Valves, *Silicon*, **2012**, *4*, 239–249 doi:10.1007/s12633-012-9119-x.

[33] Aitken, Z. H.; Luo, S.; Reynolds, S. N.; Thaulow C., Greer, J. R., Microstructure provides insights into evolutionary design and resilience of *Coscinodiscus sp*. frustule**,** *Proc. Natl. Acad. Sci.*, **2016**, *113*, 2017-2022, https://doi.org/10.1073/pnas.1519790113.

[34] Ashman, R. B., Cowin, S. C., Van Buskirk, W. C. & Rice, J. C. A continuous wave technique for the measurement of the elastic properties of cortical bone. J. Biomech. 17, 349–361 (1984). doi:10.1016/0021-9290(84)90029-0

[35] Ashman, R. B.; Cowin, S. C.; Buskirk, W. C. & Rice, J. C. A continuous wave technique for the measurement of the elastic properties of cortical bone. J. Biomech. 17, 349–361 (1984). Bansal, N. P.; Doremus R. H. Handbook of Glass Properties, Academic Press, New York, 1986

[36] Losic, D.; Rosengarten, G.; Mitchell, J. G.; Voelcker, N.H. Pore architecture of diatom frustules: Potential nanostructured membranes for molecular and particle separations, *J. of Nanosc. and Nanotech.* **2006**, *6(4),* 1-8.

[37] Xie, K., Chen M., Li, Z. A semi-analytical method for vibration analysis of thin spherical shells with elastic boundary conditions, *J. of Vibroeng.*, **2017**, *19*, 2312-2330. https://doi.org/10.21595/jve.2016.17154

[38] Shojaee, S.; Izadpanah, E.; Valizadeh, N.; Kiendl, J., Free vibration analysis of thin plates by using a NURBS-based isogeometric approach, *Finite Elem. Anal. Des.,* **2012**, *61*, 23–34 https://doi.org/10.1016/j.finel.2012.06.005

[39] Shi, X.; Shi, D.; Li, W.L.; Wang, Q., A unified method for free vibration analysis of circular, annular and sector plates with arbitrary boundary conditions, *J. Vib. Control*, **2016**, *22*, 442–456 https://doi.org/10.1177/1077546314533580

[40] Shang, X Exact solution for free vibration of a hermetic capsule, *Mech. Res. Com.*, **2001**, 28(3), 283-288 https://doi.org/10.1016/S0093-6413(01)00175-6